4 RESULTS AND DISCUSSION

4.1 *in silico* prediction of mRNA targets of reported sRNAs in *Pseudomonas aeruginosa* PAO1

Increasing number of sRNAs is being identified as a result of advancement in the field of bioinformatics and techniques like RNA-seq, tiling microarrays, etc. However, identification of mRNA targets for these sRNAs is a challenge due to the imperfect, non-contiguous base pairing between sRNAs and their targets which makes it difficult to distinguish between a true RNA-RNA hybrid and a random interaction between two RNA transcripts (Pain et al. 2015). Therefore, a number of online prediction programs like RNA Predator, Target RNA1 and IntaRNA were used to predict putative targets of sRNAs reported by (Livny et al. 2006;Sonnleitner et al. 2008) in *P. aeruginosa* strain PAO1. Out of the predicted targets, mRNA targets were selected for wet lab studies based on their region of interaction with sRNA, P value or Z score of interaction, binding energy of the sRNA-mRNA hybrid, and a continuous stretch of at least 6-8 base pairs in the interaction (Gottesman and Storz 2011). A list of predicted targets of analysed sRNAs is given in table 12.

Table 12: A list of putative targets of reported sRNAs in *P. aeruginosa* PAO1

sRNA	Target mRNAs	P value/Z score	Energy
P1	probable glutamine amidotransferase	3.53036e-07	-125
	probable short-chain dehydrogenase	0.000561549	-81
	hypothetical protein	0.000663944	-80
	UDP-3-O-acyl-N-acetylglucosamine deacetylase	0.000663944	-80
	hypothetical protein	0.00181333	-74
	hypothetical protein	0.00253426	-72
	urease accessory protein UreG	0.00299582	-71
	hypothetical protein	0.0035413	-70
	hypothetical protein	0.00418589	-69
	hypothetical protein	0.00494752	-68
P5	probable acetate kinase	3.88284e-06	-95
	hypothetical protein	0.000511226	-70
	metalloprotease secretion protein	0.000621401	-69
	general secretion pathway protein F	0.000918065	-67
	polyhydroxyalkanoate synthesis protein PhaF	0.000918065	-67
	hypothetical protein	0.00135626	-65
	probable ATP-binding component of ABC transporter	0.00135626	-65
	hypothetical protein	0.00295888	-61
	molybdopterin converting factor, small subunit	0.00295888	-61
	probable transcriptional regulator	0.00295888	-61
P7	probable acetyltransferase WbpD	0.00011609	-85
	poly(3-hydroxyalkanoic acid) synthase 2	0.00068966	-75
	hypothetical protein	0.00117684	-72
	hypothetical protein	0.00140626	-71

	nitrate-inducible formate dehydrogenase, beta subunit	0.00200784	-69
	probable transcriptional regulator	0.00286639	-67
	probable permease of ABC transporter	0.0034246	-66
	hypothetical protein	0.0040913	-65
	hypothetical protein	0.00488747	-64
	geranyltranstransferase	0.00583813	-63
P8	hypothetical protein	0.00251113	-63
	AMP nucleosidase	0.00304073	-62
	hypothetical protein	0.00445777	-60
	hypothetical protein	0.00445777	-60
	hypothetical protein	0.00539681	-59
	hypothetical protein	0.00653301	-58
	hypothetical protein	0.00653301	-58
	probable ATP-dependent RNA helicase	0.00790746	-57
	hypothetical protein	0.00790746	-57
	hypothetical protein	0.00956968	-56
P9	flagellar hook-basal body complex protein FliE	0.000567913	-77
	probable glycosyl transferase	0.000963036	-74
	hypothetical protein	0.00114838	-73
	hypothetical protein	0.00163284	-71
	hypothetical protein	0.00163284	-71
	hypothetical protein	0.00232144	-69
	probable two-component sensor	0.00276785	-68
	probable pili assembly chaperone	0.00329996	-67
	ATP synthase gamma chain	0.00393417	-66
	probable transcriptional regulator	0.00468998	-65
P11	hypothetical protein	0.000448632	-84
	hypothetical protein	0.00141571	-77
	coproporphyrinogen III oxidase, aerobic	0.00272899	-73
	probable short-chain dehydrogenase	0.00321532	-72
	polyhydroxyalkanoate synthesis protein PhaF	0.00321532	-72
	hypothetical protein	0.0044628	-70
	hypothetical protein	0.00525729	-69
	probable oxidoreductase	0.00525729	-69
	hypothetical protein	0.00619279	-68
	hypothetical protein	0.00729413	-67
P15	hypothetical protein	0.000399424	-86
	hypothetical protein	0.000551967	-84
	exoenzyme S synthesis protein B	0.000762744	-82
	hypothetical protein	0.000896614	-81
	probable two-component sensor	0.000896614	-81
	hypothetical protein	0.00105397	-80
	probable oxidoreductase	0.0014563	-78
	hypothetical protein	0.0017118	-77
	hypothetical protein	0.00201207	-76
	hypothetical protein	0.00236495	-75
P16	hypothetical protein	0.00054501	-83
	probable heme utilization protein precursor	0.00202039	-75
	hypothetical protein	0.00202039	-75
	hypothetical protein	0.00280286	-73
	hypothetical protein	0.00388779	-71
	hypothetical protein	0.00879983	-66
P18	hypothetical protein	6.7027e-05	-96

	probable permease of ABC transporter	0.000134656	-86
	probable transport protein	0.000160312	-85
	hypothetical protein	0.000190857	-84
	probable fimbrial biogenesis usher protein	0.000270511	-82
	probable oxidoreductase	0.000383403	-80
	alkaline protease secretion protein AprE	0.000543395	-78
	probable serine/threonine-protein kinase	0.000543395	-78
	probable sigma-70 factor, ECF subfamily	0.000770124	-76
	Protease IV	-18.77	-3.44
P20	hypothetical protein	0.000164674	-94
	probable transferase	0.000361774	-89
	hypothetical protein	0.000794691	-84
	dihydrofolate reductase	0.000930121	-83
	probable short-chain dehydrogenase	0.00127411	-81
	hydrogen cyanide synthase HcnB	0.0017452	-79
	hypothetical protein	0.00204246	-78
	probable secretion protein	0.00239028	-77
	ADP-L-glycero-D-mannoheptose 6-epimerase	0.00239028	-77
	peptidyl-prolyl cis-trans isomerase FklB	0.00239028	-77
P24	hypothetical protein	0.00022548	-90
	N-acetyl-gamma-glutamyl-phosphate reductase	0.0013234	-79
	probable aromatic acid decarboxylase	0.0015543	-78
	metalloprotease secretion protein	0.00182545	-77
	RecA protein	0.00182545	-77
	probable permease of ABC transporter	0.00214384	-76
	hypothetical protein	0.0025177	-75
	hypothetical protein	0.0025177	-73
	L-serine dehydratase	0.00347203	-73
	probable oxidoreductase	0.00407703	-72
P26	hypothetical protein	0.000755311	-68
	type III secretory apparatus protein PcrD	0.00530841	-58
	probable two-component sensor	0.00644909	-57
	hypothetical protein	0.00644909	-57
	hypothetical protein	0.00644909	-57
	sodium/proton antiporter NhaB	0.00783392	-56
	hypothetical protein	0.00951468	-55
P27	50S ribosomal protein L10	2.52972e-09	-155
	hypothetical protein	5.67814e-05	-95
	L-sorbosone dehydrogenase	0.00160049	-75
	probable RND efflux transporter	0.00160049	-75
	probable MFS transporter	0.00223436	-73
	D-3-phosphoglycerate dehydrogenase	0.00311888	-71
	probable ATP-binding component of ABC transporter	0.00368463	-70
	hypothetical protein	0.00435279	-69
	hypothetical protein	0.00435279	-68
	hypothetical protein	0.00435279	-67
P28	probable pili assembly chaperone	0.0022052	-74
	para-aminobenzoate synthase component I	0.00502245	-69
	probable transcriptional regulator	0.0059202	-68
	hypothetical protein	0.0059202	-68
	hypothetical protein	0.0059202	-68
	probable porin	0.00697785	-67
	hypothetical protein	0.00697785	-67

	hypothetical protein	0.00697785	-67
	probable transcriptional regulator	0.00697785	-67
	probable lauroyl acyltransferase	0.00697785	-67
P30	hypothetical protein	0.000113975	-93
	hypothetical protein	0.000582044	-83
	heat shock protein HscA	0.000582044	-83
	glutaryl-CoA dehydrogenase	0.000949183	-80
	probable ethanolamine ammonia-lyase light chain	0.00111722	-79
	probable MFS transporter	0.00111722	-79
	hypothetical protein	0.00154773	-77
	hypothetical protein	0.00154773	-77
	cytochrome o ubiquinol oxidase subunit II	0.00214394	-75
	Alginate regulatory protein AlgQ	0.00252322	-74
P32	probable transcriptional regulator	0.00461511	-63
	hypothetical protein	0.00553354	-62
	hypothetical protein	0.00953221	-59
	probable glycosyl transferase	0.00953221	-59
P34	hypothetical protein	9.62462e-08	-145
	ATP-binding component of ABC phosphate transporter	0.000380955	-91
	hypothetical protein	0.000703542	-87
	hypothetical protein	0.00111446	-84
	thiamine monophosphate kinase	0.00111446	-84
	hypothetical protein	0.00279531	-78
	probable transcriptional regulator	0.00279531	-78
	hypothetical protein	0.00379713	-76
	hypothetical protein	0.00379713	-76
	hypothetical protein	0.00379713	-76
P35	probable chemotaxis transmembrane proton channel	2.50405e-05	-89
	secretion protein MttC	7.70993e-05	-83
	probable transmembrane sensor	9.2993e-05	-82
	probable amino acid permease	0.000196807	-78
	hypothetical protein	0.000237375	-77
	hypothetical protein	0.000286304	-76
	molybdenum transport protein ModB	0.000881286	-70
	probable 2-ketogluconate kinase	0.000881286	-70
	hypothetical protein	0.000881286	-70
	probable transmembrane sensor	0.00106287	-69
P36	hypothetical protein	0.00310274	-59
	probable transporter	0.0037923	-58
	glucose inhibited division protein B	0.0037923	-58
PhrD	hypothetical protein	0.000467375	-75
	probable flavin-containing monooxygenase	0.000467375	-75
	PmbA protein	0.000810105	-72
	probable two-component response regulator	0.000810105	-72
	TolR protein	0.00243271	-66
	citrate synthase	0.00292169	-65
	probable two-component response regulator	0.00350878	-64
	hypothetical protein	0.00421359	-63
	hypothetical protein	0.00505963	-62
	Transcriptional regulator RhlR	-16.89	-3
PhrS	hypothetical protein	7.27934e-05	-94
	probable transferase	0.000167027	-89
	hypothetical protein	0.000383224	-84

	dihydrofolate reductase	0.00045246	-83
	probable short-chain dehydrogenase	0.000630707	-81
	hydrogen cyanide synthase HcnB	0.000879142	-79
	hypothetical protein	0.00103793	-78
	probable secretion protein	0.00122538	-77
	ADP-L-glycero-D-mannoheptose 6-epimerase	0.00122538	-77
	peptidyl-prolyl cis-trans isomerase FklB	0.00122538	-77
PhrX	probable ATP-binding component of ABC transporter	0.00283706	-58
	hypothetical protein	0.00645674	-54
	ketopantoate reductase	0.00645674	-54
PhrY	toluate 1,2-dioxygenase electron transfer component	0.00017029	-90
	probable MFS transporter	0.000455632	-84
	heme exporter protein CcmA	0.000632516	-82
	hypothetical protein	0.000745237	-81
	hypothetical protein	0.00121881	-78
	hypothetical protein	0.00143594	-77
	poly(3-hydroxyalkanoic acid) depolymerase	0.00169172	-76
	probable sodium:solute symporter	0.00276591	-73
	probable transcriptional regulator	0.00276591	-73
	hypothetical protein	0.00325821	-72

Out of the above analyzed sRNAs, two sRNAs, namely PhrD and P18 were chosen for further studies as they had either major virulence factors, or regulators of pathogenicity factors, as their predicted targets. RhlR, the quorum sensing regulator of virulence genes, was selected as putative target of PhrD. *Pseudomonas* uses QS mediated regulation of virulence factors to establish successful infections in host. Expression of pathogenicity factors like elastases, pyocyanin, lectins, rhamnolipids, lipases, chitinase is under RhlR regulation (Juhas M et al. 2005). Alkaline protease secretion protein E and protease IV, major virulence factors involved in establishing acute infections, served as the targets of P18. Both these proteases have a major role to play in corneal infections. Alkaline protease degrades gamma interferon and tumour necrosis factor. By affecting the function of neutrophils, it helps the pathogen in escaping phagocytosis. Alkaline protease along with an elastase, reduces the phagocytic property of leucocytes against *Pseudomonas*. Protease IV degrades IgG, complement proteins, transferrin, lactoferrin (Conibear et al. 2012). Effect of the altered levels of these sRNAs on selected targets was analyzed by means of transcriptional assays, *in vivo* RNA interaction studies on reporter gene fusions, and physiological assays.

4.2 Functional characterization of PhrD, a small non-coding RNA

PhrD, a 74 nt highly conserved small RNA is predicted to have two stem-loops in its secondary structure (Figure 10) and is flanked by two hypothetical genes: PA0714 and PA0715.

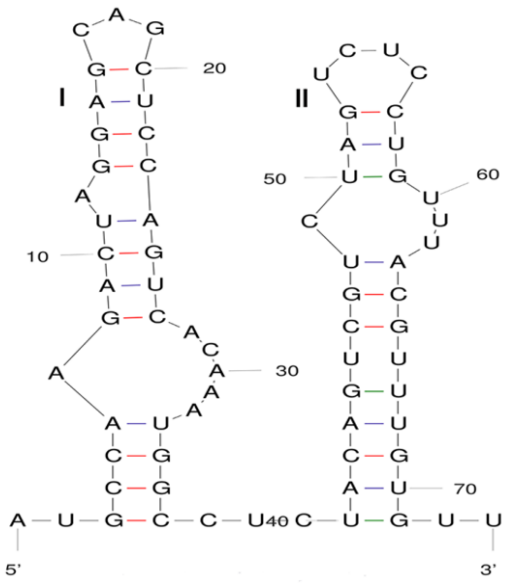

Figure 10: Secondary structure of PhrD predicted by mfold.

4.2.1 Putative targets of PhrD selected for further studies

Online programs like Target RNA1 and RNA Predator were used to determine putative targets of PhrD sRNA which were then confirmed by IntaRNA program. A list of its first 50 putative targets can be found in table 13.

Most of the predicted targets showed base pairing to the second stem (II) of PhrD (Figure 10). Out of the indicated targets, the major transcriptional activator of quorum sensing, RhlR, was chosen to study for its regulation by PhrD due to its role in quorum sensing and regulation of pathogenicity genes. *rhlR* gene reportedly has four promoters (Medina et al. 2003) (Figure 11), and the sequences coinciding with the transcription start site of the P3 promoter (downstream of P4) were predicted to bind with PhrD (-159 to -134, 'G' at position -158 being the transcription start site, Figure 12 (A)).

Table 13: A list of putative targets of PhrD in RNA Predator program

Rank	Energy (kJ/mole)	Z score[#]	Targets
1	-21.53	-4.67	major facilitator transporter
2	-21.22	-4.56	TolR protein
3	-20.54	-4.32	putative transporter
4	-19.76	-4.04	hypothetical protein PA2935
5	-19.52	-3.95	hypothetical protein PA4536
6	-19.47	-3.93	Transposase
7	-19.39	-3.9	hypothetical protein PA2777
8	-19.38	-3.9	Hcp1
9	-19.24	-3.85	hypothetical protein PA2126
10	-19.12	-3.8	DNA polymerase III subunit alpha
11	-18.98	-3.75	4-hydroxy 3-methyl but-2-enyl-diphosphate reductase
12	-18.87	-3.71	hypothetical protein PA4712
13	-18.44	-3.56	hypothetical protein PA0819
14	-18.37	-3.53	hypothetical protein PA5132
15	-18.28	-3.5	hypothetical protein PA4685
16	-17.99	-3.4	putative serine/threonine protein kinase
17	-17.99	-3.4	putative glycosyl transferase
18	-17.88	-3.36	hypothetical protein PA2462
19	-17.87	-3.35	putative glutathione peroxidise
20	-17.74	-3.31	chemotaxis specific methylesterase
21	-17.72	-3.3	hemin importer ATP binding subunit
22	-17.69	-3.29	apolipoprotein N-acyltransferase
23	-17.68	-3.29	NADH dehydrogenase subunit N
24	-17.66	-3.28	putative aminopeptidase
25	-17.62	-3.26	type III secretion system protein
26	-17.59	-3.25	hypothetical protein PA2222
27	-17.54	-3.23	pyrroloquinoline quinone biosynthesis protein F
28	-17.53	-3.23	NosY protein
29	-17.48	-3.21	multidrug efflux protein NorA
30	-17.46	-3.21	GbdR
31	-17.32	-3.16	ClpB protein
32	-17.28	-3.14	arginyl tRNA synthetase
33	-17.10	-3.08	branched chain amino acid ABC transporter permease
34	-17.08	-3.07	hypothetical protein PA1111
35	-17.02	-3.05	putative iron sulfur cluster binding protein; Rieske
36	-16.92	-3.01	PvdJ
37	**-16.89**	**-3**	**transcriptional regulator RhlR**
38	-16.81	-2.97	'two component response regulator; CopR '
39	-16.81	-2.97	4-amino 4-deoxy L-arabinose transferase
40	-16.76	-2.95	hypothetical protein PA2502
41	-16.69	-2.93	hypothetical protein PA4612
42	-16.60	-2.9	ABC transporter permease
43	-16.56	-2.88	hypothetical protein PA3127
44	-16.55	-2.88	putative oxidoreductase
45	-16.51	-2.86	major facilitator transporter
46	-16.45	-2.84	BifA
47	-16.44	-2.84	putative transcriptional regulator
48	-16.38	-2.82	transcriptional regulator
49	-16.26	-2.77	manganese transport protein MntH
50	-16.22	-2.76	hypothetical protein PA2984

Z-score is useful for comparing interactions involving different sRNAs

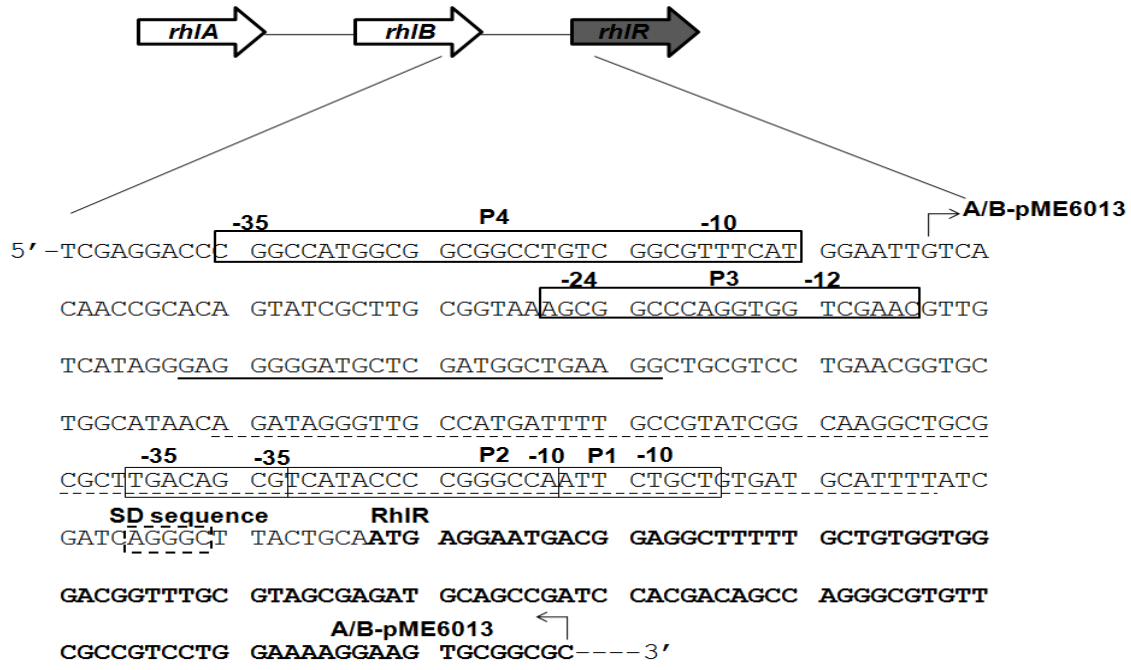

Figure 11: Schematic representation of promoter region of *rhlR* gene.
The upstream region of *rhlR* gene comprises of four promoters, P1 to P4 that are indicated by boxes. The Shine Dalgarno (SD sequence) of *RhlR* is indicated by a dotted box and the first 33 codons of *RhlR* are in bold. The PhrD interaction region is underlined by a solid line. The region comprising the P1 and P2 promoters is excluded from the translational fusion and is shown by a dotted underline. A 141 bp region comprising the P3 promoter and the interaction region was amplified by PCR and fused to the 139 bp region comprising the SD sequence and the first 33 codons to get the *rhlR::lacZ* translational fusion in the constructs A-pME6013 and B-ME6013 (with scrambled interaction sequence).

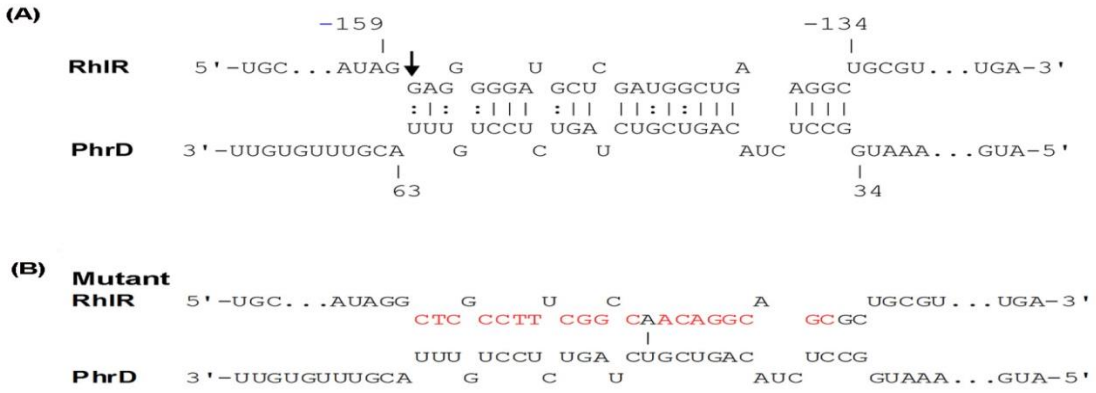

Figure 12: PhrD-*RhlR* interaction region.
(A) RNA-RNA interaction between PhrD and *RhlR*, predicted using IntaRNA program. The arrow in the beginning of interaction region indicates the transcription start site of the P3 promoter of *rhlR*. The numbers on PhrD and *RhlR* are in reference to the nucleotides from the transcription start and the translational start respectively (B) Scrambled sequence of *RhlR* PhrD interaction region incorporated in the mutant RhlR construct, B-pME6013.

4.2.2 Overexpression of PhrD from pHERD30T shuttle vector

phrD gene was amplified from *P. aeruginosa* genomic DNA with PhrD(N)F/ PhrD(N)R primers (Table 10) and a band of approximately 152 bp was obtained (Figure 13A) which was cloned in the vector pBluescript II KS(+) using *Xba*I and *Pst*I sites. The clones were confirmed by insert release by *Xba*I and *Sal*I (Figure 13B) and further with DNA sequencing at MWG Eurofins Ltd., Bangaluru. PhrD fragment was released by *Pst*I and *Xba*I digestions from pBluescript II KS(+) and sub-cloned in *Escherichia-Pseudomonas* shuttle vector pHERD30T to generate pHERD*phrD*. The clones were confirmed by insert release by *Eco*RI and *Hind*III (Figure 13C). The above constructs were made in *E. coli* DH5α as an intermediate host and were later electroporated into *P. aeruginosa* strain PAO1 (Figure 13D).

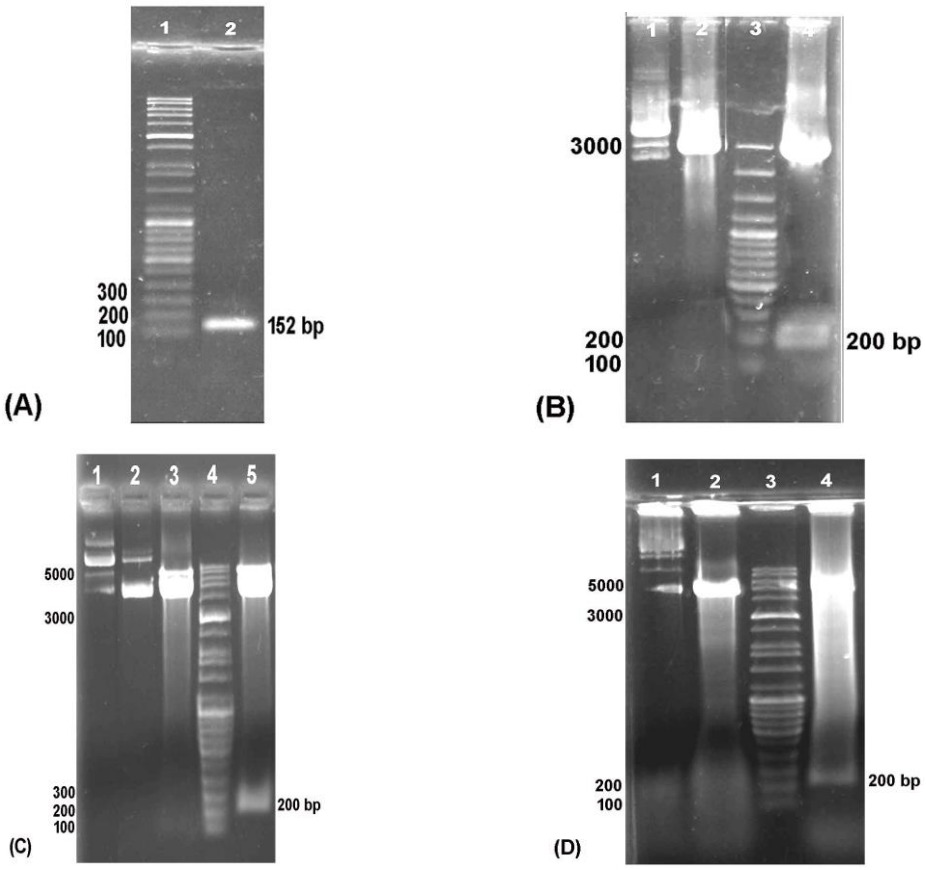

Figure 13: PCR amplification, cloning and sub-cloning of PhrD
(A) Lane 1: High range marker (100-10,000 bp), Lane 2: PhrD (152 bp). (B) Lane 1: Undigested plasmid control, Lane 2: pBSKS digested with *Sal*I/*Xba*I, Lane 3: 100 bp marker (100-3000 bp), Lane 4: pBSKS*phrD* digested with *Sal*I/*Xba*I showing an insert release of 200 bp (C) Lane 1: Undigested pHERD30T, Lane 2: Undigested pHERD*phrD*, Lane 3: *Eco*RI/*Hind*III digested pHERD30T, Lane 4: High range marker (100-10,000 bp), Lane 5: *Eco*RI/*Hind*III digested pHERD*phrD* isolated from *E.coli* DH5α showing an insert release of 200 bp. (D) Lane 1: Undigested pHERD30T, Lane 2: *Eco*RI/*Hind*III digested pHERD30T, Lane 3: High range marker (100-10,000 bp), Lane 4: *Eco*RI/*Hind*III digested pHERD*phrD* isolated from *P.aeruginosa* PAO1 showing an insert release of 200 bp.

4.2.3 Disruption of *phrD* chromosomal copy with gentamicin resistance marker

A disruption mutant of *phrD* in *P.aeruginosa* PAO1 was created by insertion of a gentamicin resistance gene (Gm) in *phrD* by homologous recombination. The *phrD* gene disruption cassette (GDC), generated by a 3-step PCR protocol depicted in Figure 14 was cloned in a plasmid followed by electroporation of the recombinant plasmid in PAO1 harbouring the recombinase proficient vector pUCP18-*RedS* to get the double-crossover mutants.

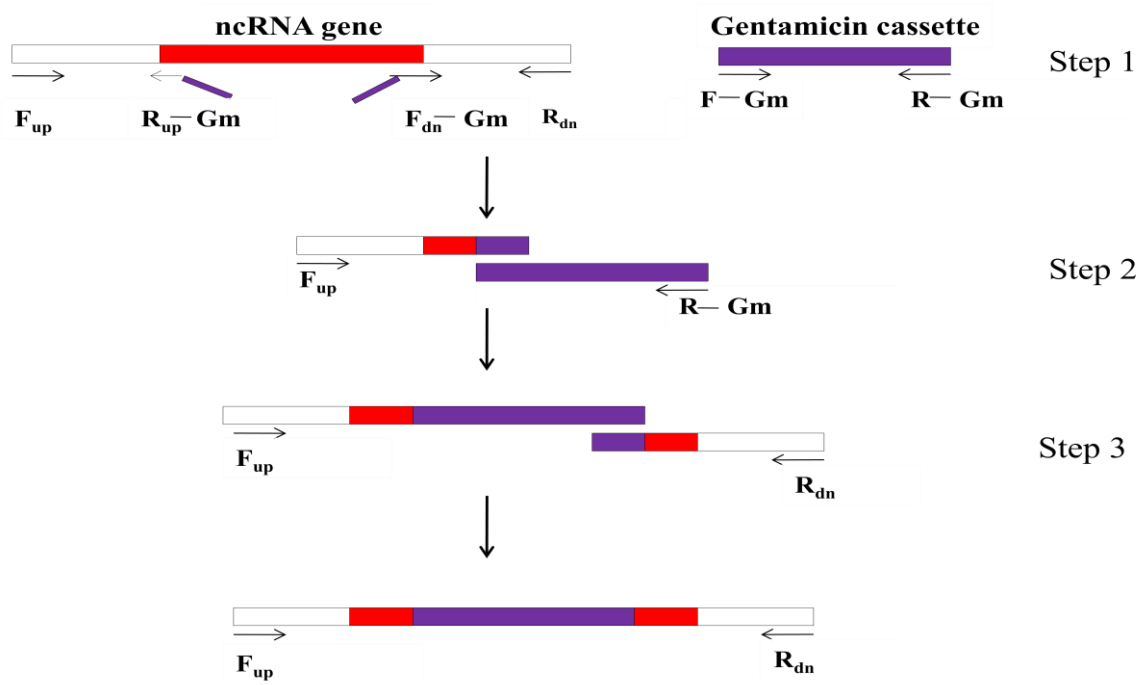

Figure 14: Pictorial representation of 3-step PCR to generate gene disruption cassette.

Amplicons of size 714 bp and 792 bp for the upstream and downstream regions of *phrD* containing the 5' and 3' end of the gene respectively and 855 bp long gentamicin marker (Figure 15A) were obtained by PCR. These were then joined together by an overlap extension PCR to obtain a 2385 bp long *phrD* gene GDC (Figure 15B). The *phrD* disruption cassette thus obtained was ligated with plasmid pTZ57R/T with 3' dT overhangs as per the manufacturer's instructions (InsTAclone PCR Cloning Kit, Fermentas). The clones were confirmed by insert release using *Eco*RI and *Hind*III (Figure 15C).

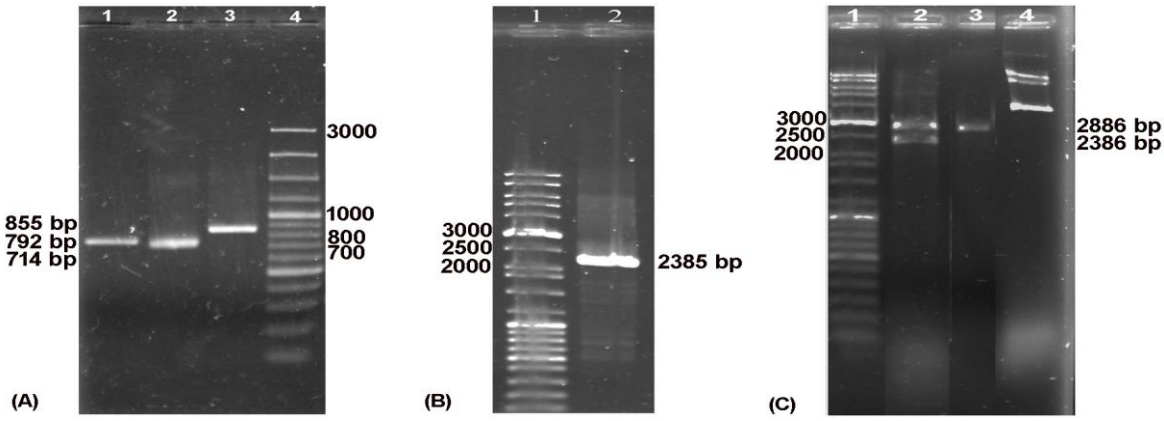

Figure 15: Construction of *phrD* gene disruption cassette
(A) Lane 1: PhrD downstream region (792 bp), Lane 2: PhrD upstream region (714 bp), Lane 3: gentamicin resistance gene (855 bp), Lane 4: 100 bp marker (100-3000 bp). (B) Lane 1: High range marker (100-10,000 bp), Lane 2: PhrD GDC (2385 bp). (C) Lane 1: High range marker (100-10,000 bp), Lane 2: *Eco*RI/ *Hind*III digested pPhrD-GDC showing an insert release of 2386 bp, Lane 3: *Eco*RI/*Hind*III digested pTZ57 R/T, Lane 4: Undigested pPhrD-GDC plasmid.

pPhrD-GDC vector was electroporated into pUCP18-*RedS* containing *P. aeruginosa* PAO1 to get the PAO1 *phrD*ΩGm mutants. To ascertain resolution of merodiploids, Gm^r colonies were patched for single colonies on LB-NaCl+Gm30 plates containing 10% sucrose. Gm^r colonies were patched onto carbenicillin plates. Four colonies that grew on the LB+Gm+sucrose but not on the carbenicillin plates were considered putative double-crossover disruptants and were verified by colony PCR (Figure 16) with different pairs of primers.

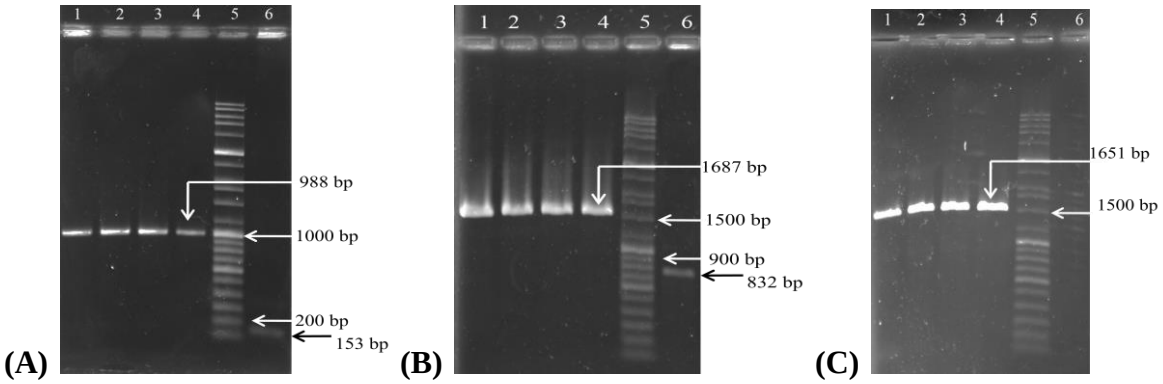

Figure 16: Confirmation of *phrD* disruption by PCR.
(A) PhrD ncRNA F/R primers; Lane 1-4: Double-crossover *phrD* mutants, Lane 5: High range marker (100-10,000 bp), Lane 6: PAO1 WT (amplicon of 153 bp from WT PhrD) (B) PhrD ncRNA F/ PhrD Dn R primers; Lane 1-4: Double-crossover *phrD* mutants, Lane 5: High range marker (100-10,000 bp), Lane 6: PAO1 WT (C) Gm F/ PhrD Dn R primers; Lane 1-4: Double-crossover mutants, Lane 5: High range marker (100-10,000 bp), Lane 6: PAO1 WT (no amplification due to absence of gentamicin casette).

4.2.4 Complementation of PAO1 *phrD*ΩGm strain with pUCP*phrD* plasmid

phrD was disrupted by a gentamicin resistance gene and *phrD* overexpression plasmid pHERD*phrD* also confers gentamicin resistance. Hence, complementation of *phrD*ΩGm was done by pUCP*phrD* that expressed *phrD* from a *lac* promoter in pUCP18 (Cb^r). *phrD* released from pHERD*phrD* was sub-cloned into *Xba*I-*Pst*I digested pUCP18 plasmid and the clones were confirmed by insert release with *Bam*HI-*Hind*III and *Pvu*II digestions (Figure 17A and B). *phrD*ΩGm strain was transformed with the above construct to get the complement strain.

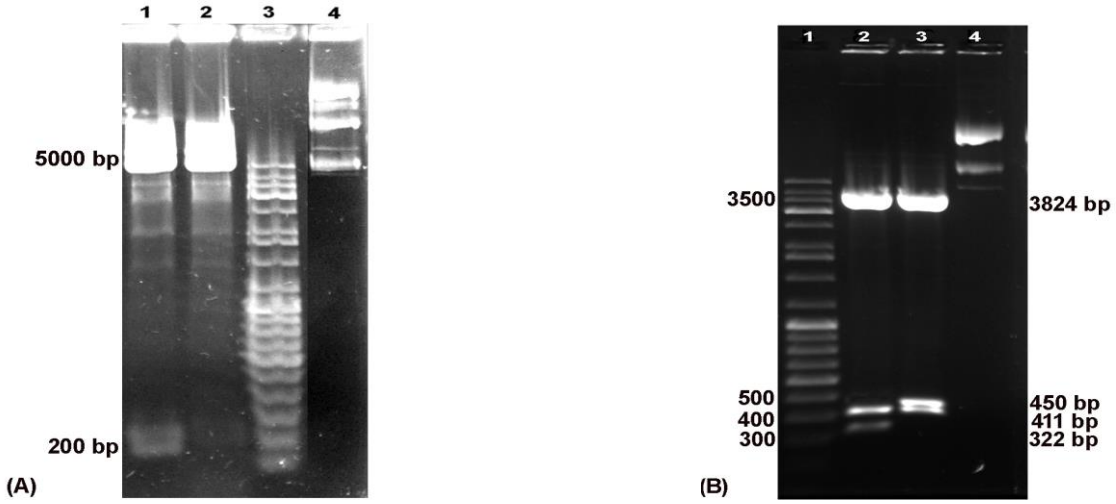

Figure 17: Sub-cloning of *phrD* into pUCP18
(A) Lane 1: pUCP*phrD* digested with *Bam*HI/ *Hind*III showing an insert release of approximately 200 bp, Lane 2: pUCP18 digested with *Bam*HI/ *Hind*III, Lane 3: Medium range marker (100-5000 bp), Lane 4: Undigested control plasmid. (B) Lane 1: Medium range marker (100-5000 bp), Lane 2: *Pvu*II digested pUCP18 plasmid, Lane 3: *Pvu*II digested pUCP*phrD* plasmid showing a band of 450 bp instead of 320 bp as seen in the control, Lane 4: Undigested control plasmid.

4.2.5 Construction of P3-*rhlR::lacZ* translational fusions

In order to create *rhlR::lacZ* translational fusions, a 141 bp long sequence that includes the P3 promoter and the PhrD interaction region of *RhlR* was amplified (primer pair AM_101 and AM_102) and fused to a 139 bp long 5'UTR region with RBS and the first 33 codons of *RhlR* mRNA (primers AM_103 and AM_104), by overlap extension PCR (Figure 18A and B). The PCR fragment was fused to the eighth codon of *lacZ* at *Eco*RI-*Pst*I digested pME6013 to get translational fusion of *rhlR* with *lacZ*, A-pME6013. A similar construct B-pME6013 that served as a negative control was made wherein the interaction region was substituted with a commercially synthesized scrambled sequence (primers AM_111 and AM_112) (Figure 18C).

Both the above constructs were confirmed by *Eco*RV digestions (Figure 18D and E). Neither of these constructs included the P4, P2 and P1 promoters mentioned by Medina and colleagues.

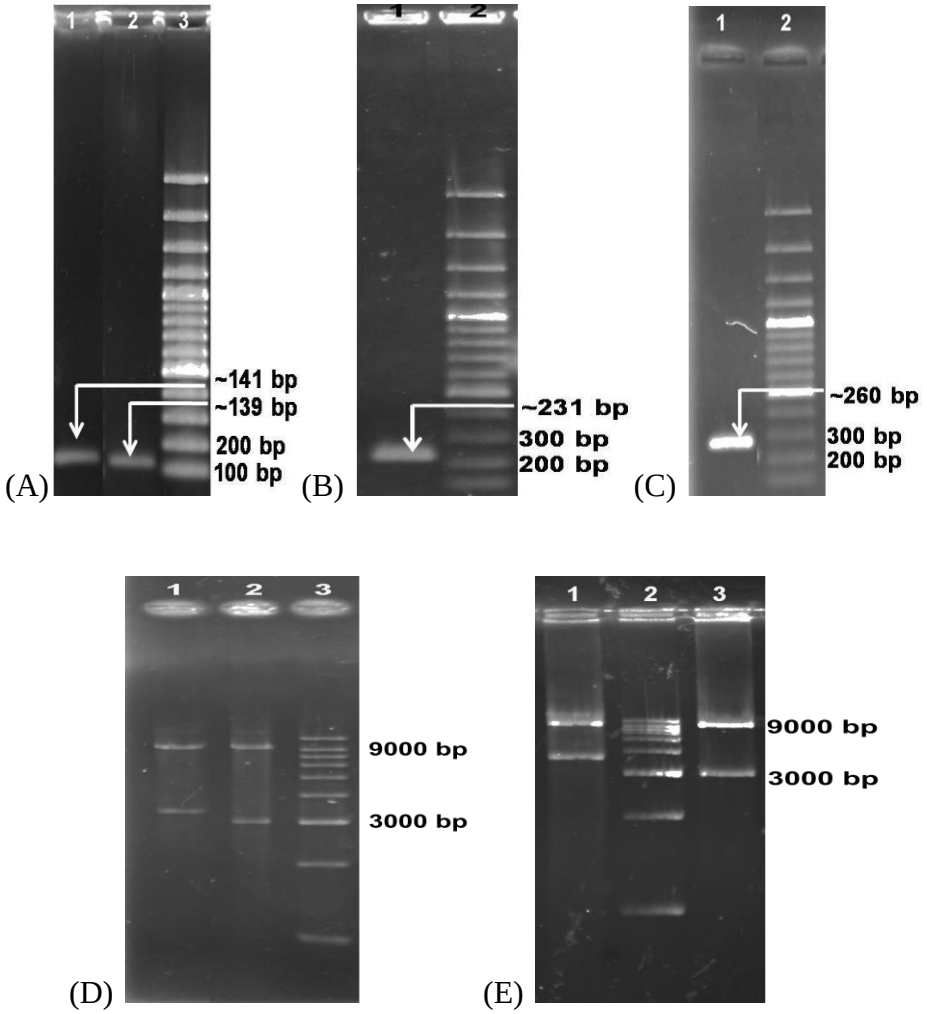

Figure 18: Construction of *rhlR::lacZ* fusions
(A) Lane 1: P3 promoter and intact interaction region amplicon (~141 bp), Lane 2: RBS and first 33 codons of *RhlR* mRNA (~139 bp), Lane 3: Medium range marker (100-5000 bp). (B) Lane 1: P3 promoter fused to the RBS of *RhlR* mRNA (~260 bp), Lane 2: Medium range marker (100-5000 bp). (C) Lane 1: P3 promoter and scrambled interaction region amplicon fused to the RBS of *RhlR* mRNA (~231 bp), Lane 2: Medium range marker (100-5000 bp). (D) Lane 1: *Eco*RV digested A-pME6013 fusion plasmid, Lane 2: *Eco*RV digested pME6013 plasmid, Lane 3: 1 kb ladder (1000-10,000 bp). (E) Lane 1: *Eco*RV digested B-pME6013 fusion plasmid, Lane 2: *Eco*RV digested pME6013 plasmid, Lane 3: 1 kb ladder (1000-10,000 bp).

4.2.6 Expression of *phrD* and its levels under different nutrient conditions

Expression of *phrD* in the modified strains and from the wild type under different nutrient conditions was studied by northern blots probed with double-stranded PhrD probes and qRT-

PCR. *phrD* without its promoter was overexpressed in *Pseudomonas* under the *pBAD* promoter using the shuttle vector pHERD30T. Two prominent transcripts of 160 nt and 74 nt were expressed from the cloned plasmid and the chromosomal copy respectively in comparison with the control strain (Figure 19A). The longer transcript derived from *phrD* cloned downstream to the *pBAD* promoter, was shown to base pair with *RhlR* transcript at the same nucleotides as would the chromosomal PhrD as analyzed by IntaRNA program (Appendix III). PhrD expression was higher from the endogenous promoter as compared to that of the cloned PhrD. However, the aggregated expression of PhrD from the two promoters was sufficient to analyze its effect on target gene expression. Expression analysis of *phrD* in the wild type (WT) strain indicated a steady increase along the growth curve after normalization with 16S rRNA gene (Figure 19B).

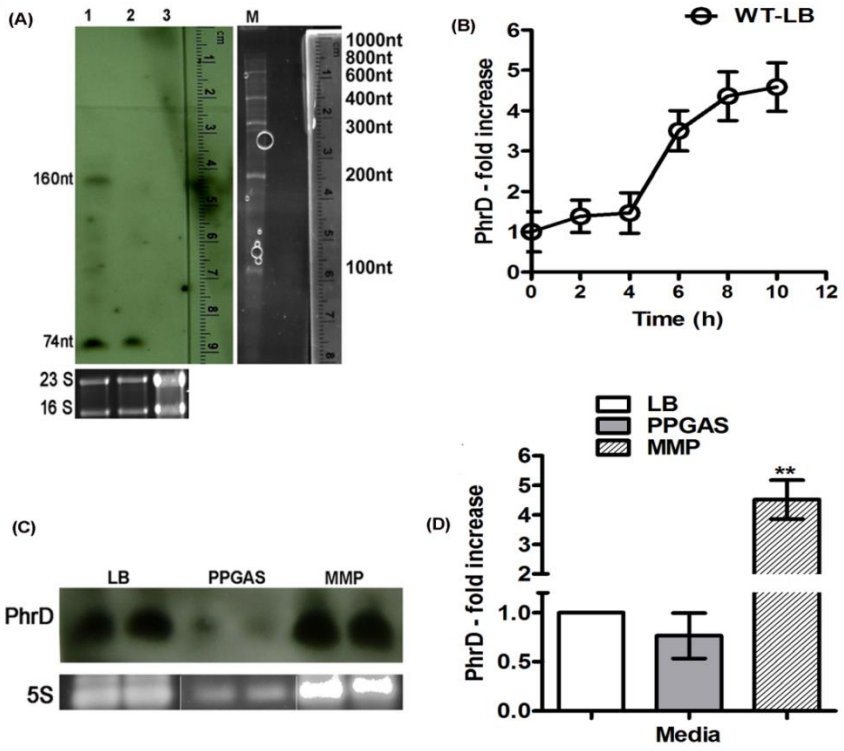

Figure 19: Expression analysis of *phrD* in *P. aeruginosa* strain PAO1
(A) Northern blots of PhrD in overexpression and disruption. Lane 1-pHERD*phrD*: overexpression; Lane 2-pHERD30T: vector control; Lane 3-*phrD*ΩGm: disruption strain. Ethidium bromide stained 23S and 16S rRNA bands on agarose gels are shown as loading controls. (B) Time course qRT-PCR of *phrD* from the WT in LB, normalized with 16S rRNA and 0 h expression as the calibrator. (C) *phrD* expression in the WT in LB, phosphate deficient PPGAS and nitrogen limited MMP media. 5S rRNA band on agarose gel is shown as the loading control. The gel has loading differences with the RNA in the PPGAS lane being poorly loaded. The two lanes of 5S rRNA used as loading control for PPGAS medium are cropped from a different gel and merged with the existing gel. (D) Comparative PhrD levels in WT under nitrogen limited MMP and phosphate limited PPGAS media compared to that in Luria broth. *phrD* expression was measured at 24 h post inoculation of PPGAS and MMP media and 5 h post inoculation of LB where in the OD_{600} was approximately 2.

Chromosomal *phrD* gene was disrupted by introduction of a gentamicin resistance gene by homologous recombination. Disruption of *phrD* was confirmed by PCR with multiple primers (Figure 16) and absence of transcript in northern blot (Figure 19A, lane 3).

PhrD was predicted to base pair with *RhlR* mRNA at the transcription start site of its σ^{54} (involved in N regulation) dependent P3 promoter which has been reported to express under phosphate limited conditions. Expression analysis of *phrD* in Luria broth, nitrogen limited MMP, and phosphate limited PPGAS medium showed that *phrD* expressed under all the studied conditions (Figure 19C) with maximum levels in MMP (5-6 fold higher than the other two) (Figure 19D).

4.2.7 PhrD positively influences *rhlR* expression

The predicted interaction region of PhrD with *RhlR* coincides with the transcription start of P3 promoter of *rhlR* gene at -159 to -134 bp upstream of the start codon of *RhlR* mRNA. *phrD* overexpression in strain PAO1 influenced a 6-fold increase on *RhlR* in qRT-PCR assays (Figure 20A). Disruption of *phrD* (*phrD*ΩGm) in PAO1 reduced *rhlR* expression to 0.2-fold while its complementation with pUCP-*phrD* restored the levels of *RhlR* (Figure 20B).

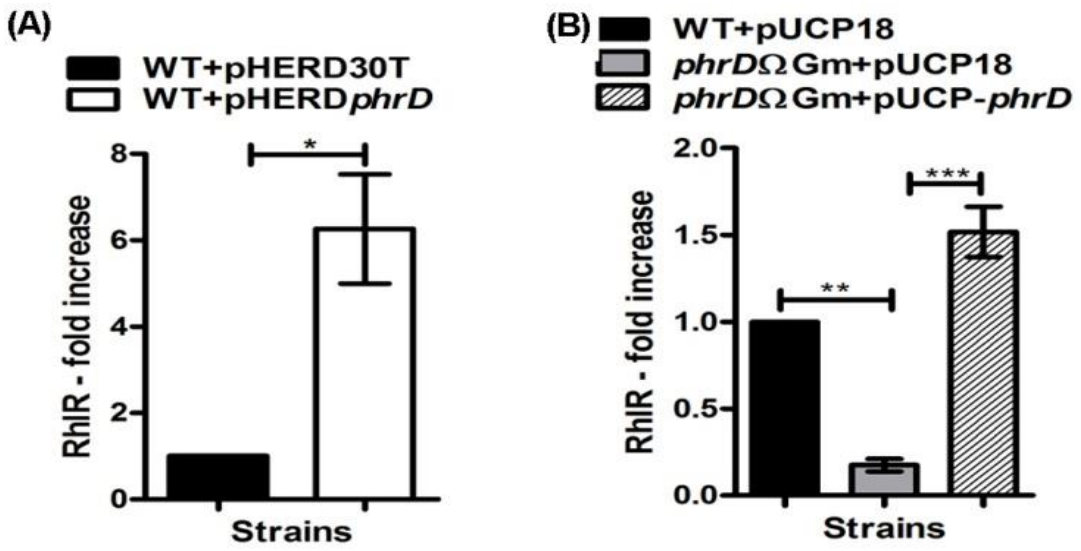

Figure 20: Effect of PhrD on *rhlR* expression.
qRT-PCR analysis of *RhlR* transcripts from cells grown in Luria broth. Two different vectors (pHERD30T and pUP18) bearing *phrD* were separately used for measurement of *RhlR* in WT background (A), and in complemented disruption (B). * indicates statistically significant data between the strains determined using Paired t test and one way ANOVA ** ($P<0.01$) in (A) and (B) respectively. The data is represented as the mean ± SD of three individual experiments and each sample was analyzed in triplicates.

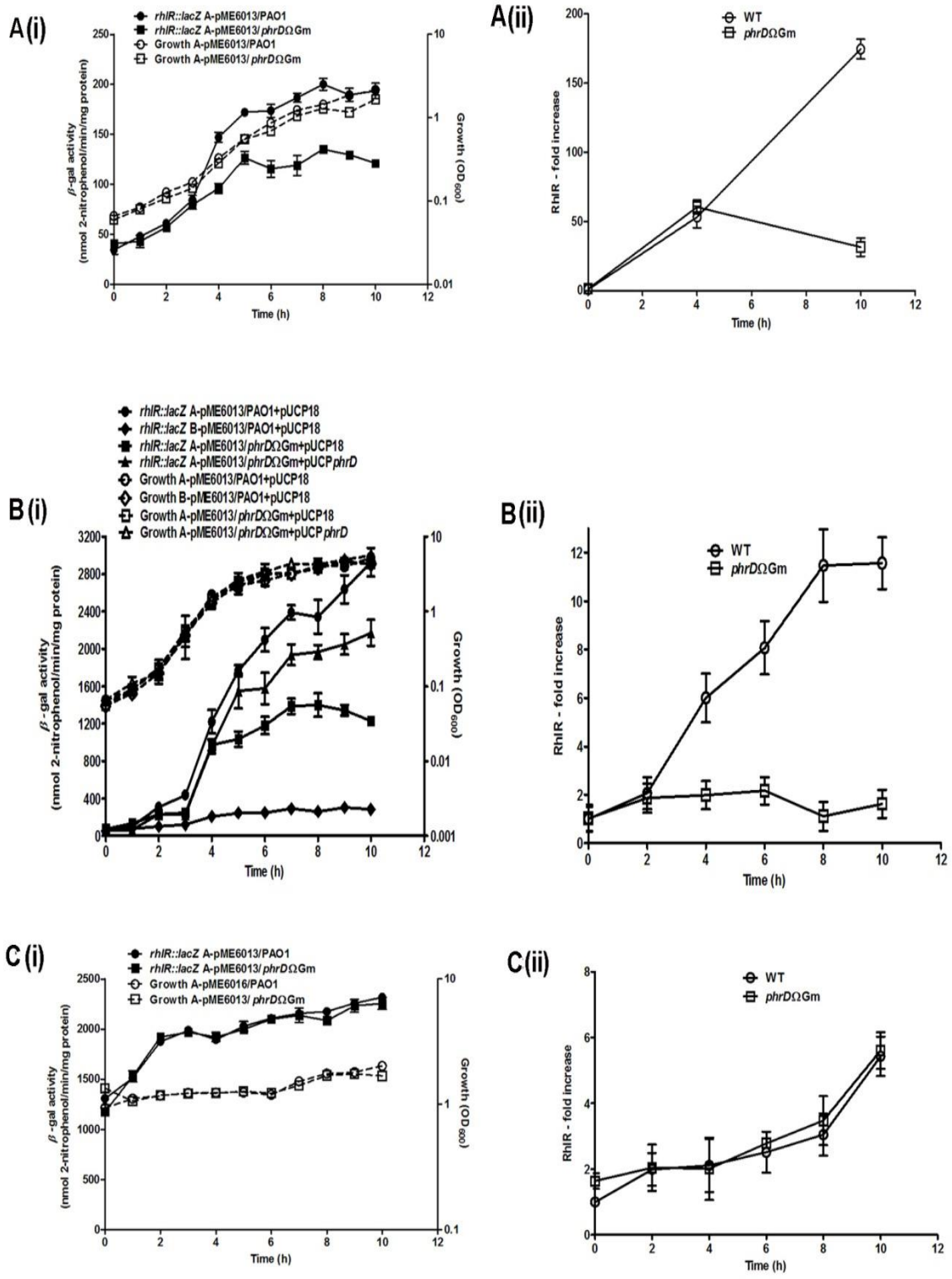

Figure 21: PhrD positively regulates *rhlR* expression in *P. aeruginosa* PAO1.
Time course measurement of *RhlR* levels by *β*-galactosidase activity of P3 *rhlR::lacZ* fusion (i), and qRTPCR (ii), measured in WT and *phrD* disruption mutant under: (A) Phosphate limited PPGAS medium (B) Luria broth (C) N-limited MMP medium. In case of MMP, the cells were first grown to the desired OD in N-rich medium and resuspended in N-limited MMP. There was no net growth due to nitrogen starvation. *β*-galactosidase activity of the disruption strain complemented with *phrD* overexpression plasmid is measured in Luria broth. The data is represented as the mean ± SD of three individual experiments and each sample was analyzed in triplicates.

With an objective of establishing a correlation between PhrD and *RhlR* levels, *lacZ* reporter translational fusions were constructed from promoter P3-*rhlR* (Figure 11, construct A-pME6013) and a time course measurement of *β*-galactosidase activity in PPGAS, LB and MMP media was correlated with *RhlR* transcript levels. *β*-galactosidase activity of the fusion exhibited a specific increase along the log phase up to 10 h in the WT and the disruption strains. The increase in WT, as compared to the disruption, was 1.5 and 2.5-fold in PPGAS and LB respectively (Figure 21 A (i) and B (i)). This paralleled with a 6-9 fold increase in the overall transcript levels of *RhlR* in the WT PAO1 with respect to the disruption in these media (Figure 21A(ii) and B(ii)). Comparing the increase observed in qRT-PCR with that of P3-*rhlR::lacZ* fusion explains that the difference in the fold increase might arise as a consequence of the modulation of transcripts arising from P4 promoter also. Complementation of the disruption strain by the cloned PhrD restored its *β*-galactosidase levels to ~ 75% of that of the WT (Figure 21B(i)). Expression of B-pME6013 bearing a nonspecific scrambled interaction sequence did not show any increase even in the WT (*phrD*+) background (Figure 21B(i)). These results corroborated the positive influence of PhrD with a sequence specific interaction to *RhlR* transcripts.

The expression of P3-*rhlR::lacZ* was very high and maximum in nitrogen limited MMP medium as compared to other media and had no difference between WT and disruption strains (Figure 21C(i)).This result perhaps indicated that under amino acid starvation there is an involvement of stringent response mediated by ppGpp in the high expression of *rhlR* (van Delden et al. 2001;Schafhauser et al. 2014) alleviating the requirement of PhrD under these conditions.

A steady increase in the transcript levels of *RhlR* in the presence of PhrD indicated its role in modulation of *rhlR* expression from P3 and P4 promoters (Fig. 21A(ii) and B(ii)). Enhancement of expression of P3-*rhlR::lacZ* fusion by PhrD, observed in PPGAS and Luria broth (Fig. 21A(i) and B(i)), signifies its role in regulation of *rhlR* expression under phosphate deficient and nutrient rich conditions. Although *rhlR* expression is reported to be dependent on LasR when grown in Luria broth (Latifi et al. 1996), above results indicate that PhrD is an additional regulator of RhlR under these conditions. PhrD had no influence on *rhlR* expression in MMP medium (Fig. 20C(i) and C(ii)), its role perhaps being overruled by stringent response under this condition. Amino acid starvation in *P. aeruginosa* promptly elicits the RelA protein-mediated stringent response (SR) that synthesizes the signalling molecule (p)ppGpp.

The QS-based response is mediated by RelA since a (p)ppGpp-null SR mutant (*spoT relA*) shows reduced *rhlI*, *rhlR*, *lasI*, and *lasR* expression (Schafhauser et al. 2014). Further, overexpression of RelA leads to the early transcription of the *lasR* and *rhlR* genes, production of QS signals, and overproduction of QS-dependent virulence factors rhamnolipids, pyocyanin, elastase, etc. (van Delden et al. 2001).

4.2.8 RhlR expression is regulated by PhrD in a heterologous system

Subsequent to the positive influence of PhrD on *rhlR* expression, the specificity of their interaction was assayed in the heterologous host *E.coli* with the constructs A-pME6013 and B-pME6013. A-pME6013 harboured the intact interaction region (Figure 12A) whereas B-pME6013 contained a scrambled stretch of the same 25 nucleotides (Figure 12B) instead of the predicted interaction region and served as a negative control. When introduced into an *E. coli* containing the PhrD overexpressing plasmid, *β*-galactosidase activity of the fusion with intact interaction region showed a specific increase of 10-fold with growth (Figure 22).

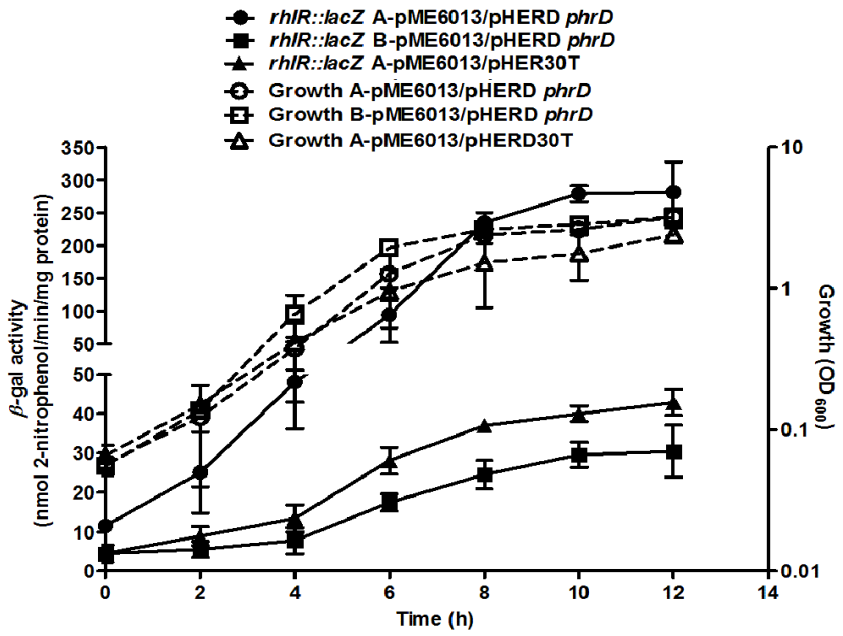

Figure 22: PhrD regulates *rhlR* in a heterologous system.
β-galactosidase activities from *rhlR::lacZ* fusion plasmids (continuous lines, filled symbols) and growth (dotted lines, open symbols) in *E. coli* cultures growing in LB at different time points. A-pME6013- fusion bearing intact PhrD interaction region; B-pME6013 - fusion with scrambled interaction region; pHERD*phrD*- *phrD* overexpression plasmid. The results are representative of three individual experiments.

No significant increase was observed in the expression of P3-*rhlR::lacZ* fusion with the scrambled PhrD-*RhlR* mRNA interaction region and in A-pME6013 with vector plasmid (no PhrD). These results proved the specific involvement and significance of base pairing interaction of PhrD with *RhlR* mRNA at the stretch of 25 nucleotides at the 5'UTR. Also, regulation of *RhlR* by PhrD in a heterologous system like *E.coli* proved that the interaction between PhrD and *RhlR* could be carried out without the assistance of any *Pseudomonas* specific proteins.

The *Pseudomonas* background however facilitated better expression of *rhlR* than *E. coli* probably owing to better recognition of P3 promoter by *Pseudomonas* sigma factors or involvement of additional *Pseudomonas* proteins. A similar *E. coli* host system was used earlier for *in vivo* identification of nucleotides important for regulation of *HapR* mRNA by Qrr sRNA of *V. cholerae* (Bardill et al. 2011).

4.2.9 PhrD positively influences rhamnolipid and pyocyanin production

RhlR, in complex with its cognate autoinducer C4-HSL, stimulates the synthesis of important virulence factors like rhamnolipids and pyocyanin pigment. Therefore, an effect on their production in relation to PhrD could be partially attributed to the regulation of *rhlR* by this small RNA. Rhamnolipids are known to be produced maximally under elevated C/N ratio under nitrogen exhaustion (Soberon-Chavez et al. 2005).

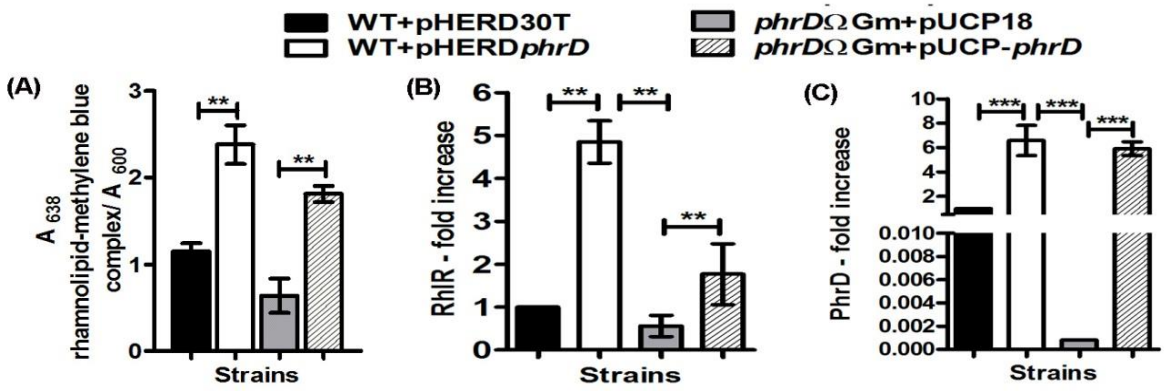

Figure 23: PhrD positively influences rhamnolipid production.
(A) Spectrophotometric assay for rhamnolipid measurement from culture supernatants by methylene blue method. Increase in rhamnolipid production is represented as increase in the absorbance at 638 nm normalized to absorbance at 600 nm of the culture. (B) and (C) *RhlR* and *PhrD* levels respectively. All these measurements were carried out in M9 medium. ** indicates statistically significant data at P<0.01 as analyzed by one way ANOVA. Each experiment was performed thrice.

Measurement of rhamnolipid levels in M9 defined medium with 0.4% glycerol and low nitrogen source (0.1 g/L KNO3) showed an increase of 2.5-fold under *phrD* overexpression (Figure 23A). The disruption strain that showed 0.5-fold level of rhamnolipid was restored to 1.8-fold when complemented with multicopy PhrD. The rhamnolipid levels in these strains are in correlation with that of *RhlR* and PhrD levels in M9 (Figure 23B and C). Likewise, the pyocyanin production in LB that was increased by 4-fold in pHERD*phrD* strain is also in correlation with the corresponding *RhlR* levels (Figure 24 and Figure 20A). Although an increase in RhlR levels, due to PhrD over expression, elevates the pyocyanin production but PhrD$^-$ may not have a marked effect on pyocyanin as PqsR is still active to maintain pyocyanin levels (Lee and Zhang 2015).

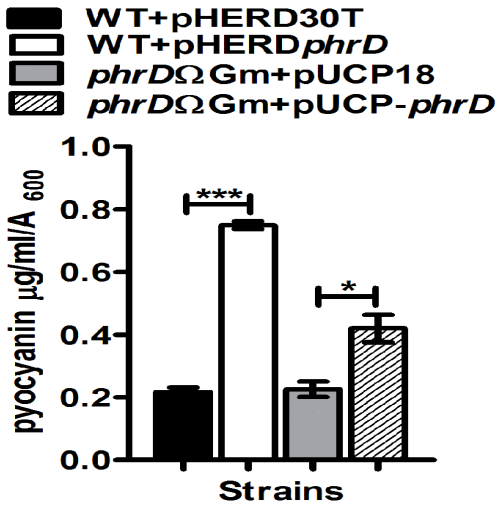

Figure 24: Pyocyanin production under altered levels of PhrD.
Pyocyanin levels in LB were measured as µg / ml /OD600 of the culture. *** and * indicates statistically significant data at P<0.001 and P<0.05, as analyzed by one way ANOVA performed on data obtained from three independent experiments.

The increase induced by PhrD in the production of rhamnolipid and pyocyanin mediated by RhlR reflected an indirect regulation of these pathogenicity factors by this sRNA (Figure 23A and 24). The haemolytic activity as well as high surface activities of rhamnolipids causes lyses of polymorphonuclear leukocytes and monocyte-derived macrophages leading to necrosis (Bjarnsholt et al. 2010). Strains lacking in rhamnolipid production are rapidly cleared from the lungs of *Pseudomonas* infected mice (Van Gennip et al. 2009). Pyocyanin influences pathogenicity by causing goblet cell metaplasia and hyperplasia, airway fibrosis, and alveolar

airway destruction in cystic fibrosis lungs (Caldwell et al. 2009). It damages human cells by causing inhibition of cellular respiration, ciliary function, epidermal cell growth, prostacyclin release and disruption of calcium homeostasis (Lau et al. 2004). PhrD-directed increase in the synthesis of these RhlR associated virulence factors may enhance invasiveness and colonization of the pathogen.

4.2.10 Significance of PhrD sRNA in *P. aeruginosa*

Bacterial small RNAs have a crucial role to play in general physiology (Papenfort and Vogel 2014), pathogenicity (Reinhart et al. 2015), quorum sensing (Feng et al. 2015), and combating environmental stresses (van der Meulen et al. 2017). This work establishes PhrD sRNA as a regulator of quorum sensing in *P. aeruginosa* under different nutrient conditions that mimic host physiology thereby assisting this bacterium to tune in to the environmental and host induced stimuli.

PhrD regulates quorum sensing under different conditions in *P. aeruginosa* unlike other previously characterized sRNAs: RsmY regulates *rhl* system under nutrient rich conditions (Kay et al. 2006). PhrS activates PqsR quorum sensing regulator under oxygen limited conditions leading to increased pyocyanin production (Sonnleitner et al. 2011). Base pairing of NrsZ sRNA with *rhlA* activates rhamnolipid production under nitrogen limitation (Wenner et al. 2014) whereas PhrD enhances both, rhamnolipid and pyocyanin production, by positively influencing RhlR.

Expression of sRNAs is mostly tightly regulated and they express under specific growth or nutrient conditions like oxidative stress (Gelsinger and DiRuggiero 2018), glucose- phosphate stress (Bobrovskyy and Vanderpool 2016), iron limitation (Ghosh et al. 2017), etc. On the other hand, PhrD sRNA studied here was found to express under several conditions including nutrient rich (Luria broth), phosphate deficient (PPGAS), and N-limited conditions (MMP). These results find implications in the role of PhrD in colonization and sustainability of *Pseudomonas aeruginosa*. In addition to the nutrient rich niches inside the host such as mucus of CF patients and soft tissues (Folkesson et al. 2012;Turner et al. 2014), *P. aeruginosa* undergoes a shift from a nosocomial colonizing pathogen to a lethal one when it senses phosphate deprivation post an acute surgical injury (Long et al. 2008). This is achieved by RhlR mediated induction of rhamnolipid and pyocyanin production in a PhoB dependent manner (Jensen et al. 2006). The influence of PhrD on the expression of *rhlR* under phosphate starvation may implicate enhanced QS via deployment of regulatory network of genes expressed under phosphate deprivation.

PhrD leads to increase in *rhlR* expression and synthesis of rhamnolipids and pyocyanin, its downstream pathogenicity factors. Rhamnolipids regulated by RhlR play a major role in the maintenance of biofilms. They inhibit adhesion between the cells and blocking of water and oxygen channels by preventing biomass accumulation in the channels (Vinckx et al. 2010). Biofilms formed by *Pseudomonas* are important as they give protection against antibiotics, nutrient deprivation, oxygen deficit, acid and pH stress (Wood et al. 2018). The virulence of *P. aeruginosa* is majorly mediated via secreted factors (van 't Wout et al. 2015) and pyocyanin is emerging as an important factor among them (Hall et al. 2016). This redox active pigment secreted profusely in lungs of cystic fibrosis patients (Lau et al. 2004) was found to affect respiratory, cardiovascular, urological, and central nervous systems, *in vitro* (Hall et al. 2016). Pyocyanin deficient mutants were found to be less deleterious than the wild type strains (Lau et al. 2004). Cytotoxic effects of pyocyanin cause autophagy and apoptosis of host cells (Qadri et al. 2016). Thus, it can be said that PhrD may make this opportunistic pathogen more challenging to deal with by facilitating its survival, colonization, and sustenance during host-pathogen interaction.

Taken together, this work demonstrates an additional route of positive regulation of the quorum sensing circuit in *P. aeruginosa* by the small regulatory RNA PhrD via RhlR, the transcriptional activator of several virulence factors of this opportunistic human pathogen.

4.3 Functional characterization of P18, a small non-coding RNA

P18, an approximately 135 nt long sRNA reported in *P. aeruginosa* strain PAO1 (Livny et al. 2006), is flanked by two hypothetical genes *viz.* PA3304 and PA3305 and is characterized by the presence of four stem-loops in its secondary structure (Figure 25) as predicted by mfold.

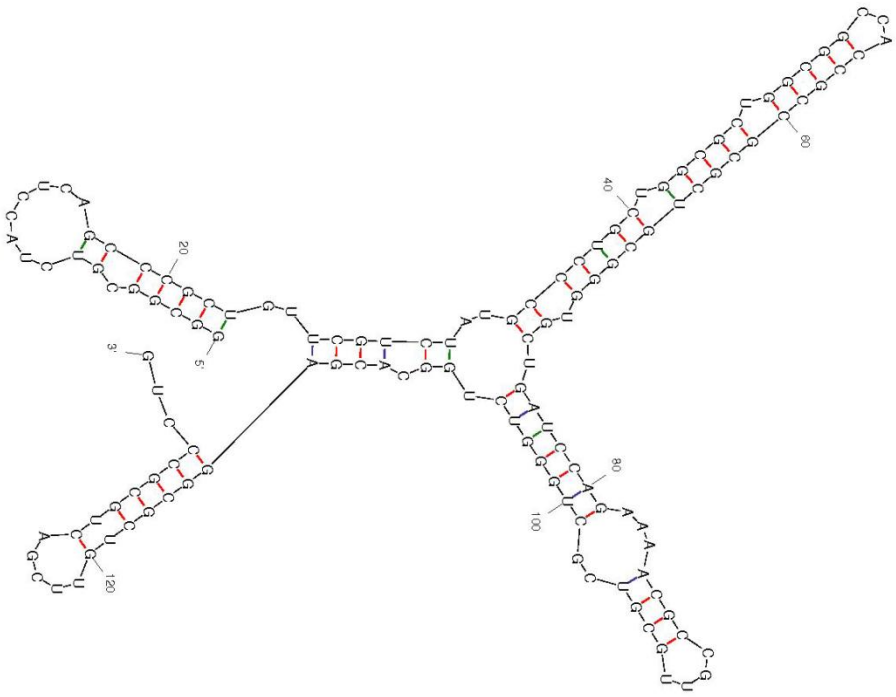

Figure 25: **Secondary structure of P18 predicted by mfold.**

4.3.1 Putative targets of P18 selected for further studies

Putative targets of the sRNA were predicted using Target RNA1 and RNA Predator program and confirmed using IntaRNA program. A list of potential targets of P18 is given in table 14. Out of the predicted targets, alkaline protease secretion protein E (*AprE*) and protease IV (*Piv*) were selected for further studies. *aprE* encodes a membrane fusion protein, which is a part of type I secretion system and facilitates secretion of alkaline protease. Alkaline protease, a zinc metalloprotease, degrades C2 component of host complement system hindering complement mediated phagocytosis and bacterial clearance (Laarman et al. 2012). *piv* encodes a lysine endoprotease, which degrades various host proteins like plasminogen,

Table 14: A list of putative targets of P18

Rank	Energy (kJ/mole) / Score	Z score / P value	Targets
Targets as predicted by RNA Predator			
1	-21.46	-4.43	ABC transporter ATP binding protein
2	-21.05	-4.30	hypothetical protein PA3081
3	-20.09	-4.27	putative heme utilization protein precursor
4	-20.55	-4.13	hypothetical protein PA4704
5	-20.52	-4.12	hypothetical protein PA3598
6	-19.74	-3.86	putative transcriptional regulator
7	-19.70	-3.85	putative transcriptional regulator
8	-19.50	-3.79	putative glycerol 3 phosphate acyltransferase PlsX
9	-19.40	-3.75	putative oxidoreductase
10	-19.35	-3.74	hypothetical protein PA0788
11	-19.35	-3.74	putative chemotaxis transducer
12	-19.21	-3.69	2 aminoethylphosphonate pyruvate transaminase
13	-19.02	-3.63	putative oxidoreductase
14	-18.96	-3.61	putative ClpA/B type protease
15	-18.87	-3.58	hypothetical protein PA1427
16	-18.66	-3.51	threonine dehydratase
17	-18.61	-3.49	putative transcriptional regulator
18	-18.56	-3.47	aldehyde dehydrogenase
19	**-18.47**	**-3.44**	**protease IV**
20	-18.43	-3.43	hypothetical protein PA1572
Targets as predicted by Target RNA 1			
1	-90	6.7027e-05	hypothetical protein
2	-86	0.00013465	probable permease of ABC transporter
3	-85	0.00016031	probable transport protein
4	-84	0.00019085	hypothetical protein
5	-82	0.00027051	probable fimbrial biogenesis usher protein
6	-80	0.00038340	probable serine/threonine-protein kinase
7	**-78**	**0.00054339**	**alkaline protease secretion protein Apr E**
8	-78	0.00054339	probable serine/threonine-protein kinase
9	-76	0.00077012	probable sigma-70 factor, ECF subfamily
10	-76	0.00077012	probable two-component sensor

P value is determined for a sRNA: mRNA hybridization by determining the probability of observing a score by chance, equal to or less than the given sRNA:mRNA hybridization score. The parameters used for prediction include P-value threshold of ≤ 0.05, with the hybridization seed of 8, GU base pairs allowed and the targets are tabulated in the decreasing order of significance. Z-score is useful for comparing interactions involving different sRNAs. Energy score is the energy of interaction needed for hybridization and is corrected for opening of secondary structures in both the RNA species.

fibrinogen, complement, immunoglobulins and surface proteins (Smith et al. 2006;Mochizuki et al. 2014;Oh et al. 2017). Both, alkaline protease and protease IV, cause microbial keratitis and have a significant role to play in corneal and lung infections (Hobden 2002;Tang et al. 2013). P18 interacts with *Piv* and *AprE* mRNAs in the coding region and 5'UTR respectively as depicted in Figure 26.

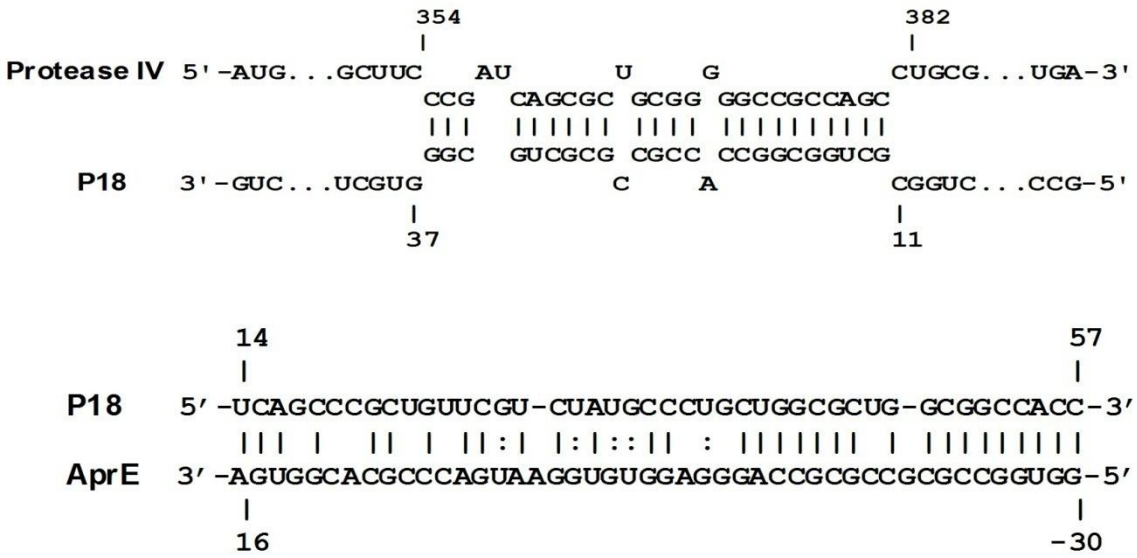

Figure 26: RNA-RNA interaction of P18 sRNA with target mRNAs.
The numbers on P18 and the target mRNAs are in reference with the transcription and translational start site respectively.

While the gene encoding Protease IV (*piv*) is an independent transcription unit, *aprE*, *i.e.* the gene expressing alkaline protease secretion protein E, is part of aprX-aprD-aprE-aprF operon (Figure 27).

Figure 27: Genetic organization of *aprE* in PAO1 genome.
Function of *aprX* is unknown. *aprD* and *aprE* encode cytoplasmic membrane proteins while *aprF* codes for outer membrane protein. *aprA* codes for alkaline metalloproteinase precursor.

4.3.2 Overexpression of P18 from pHERD30T shuttle vector

In order to clone the sRNA under an inducible promoter from a plasmid and to isolate a promoter-less gene, an extensive search for a promoter was carried out in the region spanning up to 1 kb upstream from the reported start coordinate, using several online programs like Softberry's BPROM (http://www.softberry.com/berry.phtml?topic=bprom&group=programs&subgroup=gfindb), Virtual footprint (http://www.prodoric.de/vfp/vfp_promoter.php), PePPER

(http://genome2d.molgenrug.nl), etc. However, the promoter of P18 sRNA could not be determined. Rho-independent transcriptional terminator of P18 was determined using ARNold web tool. Therefore, the region spanning from the start coordinate reported by (Livny et al. 2006) to the predicted transcriptional terminator was amplified from *P. aeruginosa* genomic DNA with P18(F)APM/P18(R)APM primers (Table 10). A band of 184 bp was obtained (Figure 28A) and cloned in the vector pBluescript II KS(+) using *Xba*I and *Pst*I sites. The clones were confirmed by insert release (Figure 28B) and by DNA sequencing. Further P18 was sub-cloned at *Xba*I-*Pst*I sites in *Escherichia-Pseudomonas* shuttle vector pHERD30T to generate pHERD*p18*. The clones were confirmed by insert release by *Eco*RI and *Hind*III (Figure 28C). The above constructs were made in *E. coli* DH5α as an intermediate host and were later electroporated into *P. aeruginosa* strain PAO1 (Figure 28D).

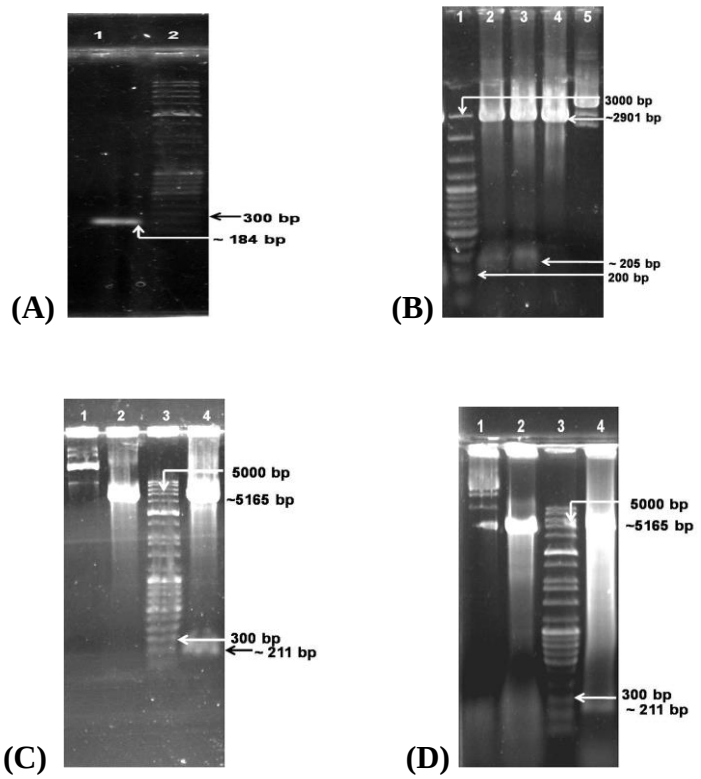

Figure 28: PCR amplification, cloning and sub-cloning of P18.
(A) Lane 1: P18 (184 bp), Lane 2: High range marker (100-10,000 bp). (B) Lane 1: 100 bp marker (100-3000 bp), Lane 2 and Lane 3: An insert release of ~205 bp from pBSKS*p18* digested with *Sal*I/*Xba*I, Lane 4: pBSKS digested with *Sal*I/*Xba*I, Lane 5: Undigested plasmid control. (C) Lane 1: Undigested pHERD30T, Lane 2: *Eco*RI/*Hind*III digested pHERD30T, Lane 3: High range marker (100-10,000 bp), Lane 4: An insert release of 211 bp from *Eco*RI/*Hind*III digested pHERD*p18* isolated from *E.coli* DH5α. (D) Lane 1 :Undigested pHERD30T, Lane 2: *Eco*RI/*Hind*III digested pHERD30T, Lane 3: High range marker (100-10,000 bp), Lane 4: An insert release of 211 bp from *Eco*RI/*Hind*III digested pHERD*p18* isolated from *P.aeruginosa* PAO1.

4.3.3 Disruption of *p18* chromosomal copy

p18 gene was disrupted in *P. aeruginosa* PAO1 as described in the section 4.2.3. Amplicons of size 657 bp and 556 bp from the upstream and downstream regions of *p18* respectively and 855 bp long gentamicin resistance gene (Figure 29A and B) were obtained by PCR. These were then joined together by an overlap extension PCR to obtain a 2068 bp long *p18* gene disruption cassette (GDC) (Figure 29C). The *p18* disruption cassette thus obtained was ligated into *Eco*RV digested pBSKS. The clones were confirmed by insert cut using *Eco*RI (Figure 29D).

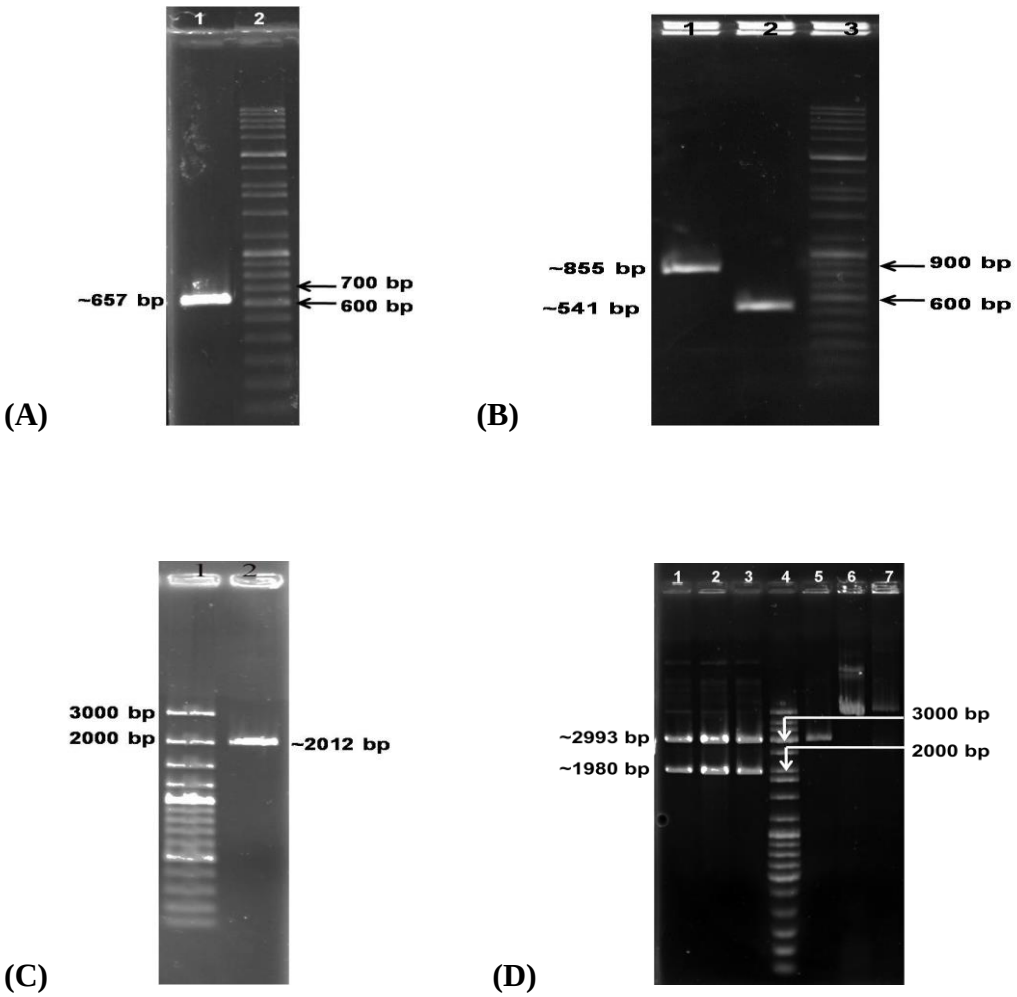

Figure 29: Construction of *p18* gene disruption cassette.
(A) Lane 1: P18 upstream region (657 bp), Lane 2: High range marker (100-10,000 bp). (B) Lane 1: Gentamicin resistance gene (855 bp), Lane 2: P18 downstream region (541 bp), Lane 3: High range marker (100-10,000 bp). (C) Lane 1: 100 bp marker (100-3000 bp), Lane 2: P18 GDC (2012 bp) .(D) Lane 1,2,3: *Eco*RI digested p*p18*-GDC, Lane 4: Medium range marker (100-5,000 bp), Lane 5: *Eco*RI digested pBSKS, Lane 6: Undigested p*p18*-GDC plasmid, Lane 7: Undigested pBSKS.

p*p18*-GDC vector was electroporated in *P.aeruginosa* PAO1 containing pUCP18-*RedS* (λ recombinase) to get the PAO1 *p18*ΩGm mutants. To ascertain resolution of merodiploids, Gm^r colonies were streaked for single colonies on LB-NaCl plates containing 10% sucrose and gentamicin. Gm^r colonies from these plates were patched onto LB plates with carbenicillin. The one colony that grew on gentamicin+sucrose plates but not on the carbenicillin plates was considered to be the double-crossover disruptant and verified by colony PCR with different pairs of primers (Figure 30).

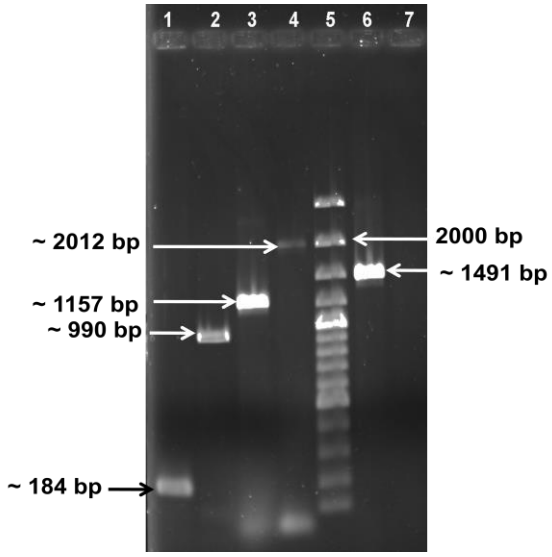

Figure 30: Confirmation of *p18* disruption by PCR using 3 sets of primers.
P18 ncRNA F/R primers; Lane 1: PAO1 WT (amplicon of ~184 bp from WT P18), Lane 2: Double-crossover *p18* mutant (~990 bp). Flanking primers; Lane 3: PAO1 WT (amplicon of ~1157 bp), Lane 4: Double-crossover *p18* mutant (~2012 bp). Lane 5: 100 bp marker (100-3,000 bp). Upstream Fwd/Gm Rev primers; Lane 6: Double-crossover mutant (~1491 bp), Lane 7: PAO1 WT (no amplification).

4.3.4 Expression analysis of P18 sRNA

A promoter for P18 sRNA could not be detected using online programs. Therefore, the complete 135 nt sequence of P18 reported by (Livny et al. 2006) along with the predicted terminator was cloned under the arabinose inducible *pBAD* promoter in the *E. coli-Pseudomonas* shuttle vector pHERD30T. The chromosomally expressed 100 nt transcript as reported in (Livny et al. 2006) was not observed in northern blots. However, an expected 257 nt transcript generated from the vector-borne promoter was observed in the overexpression strain (Figure 31A, lane 2).

Expression of P18 was 6-fold higher in the overexpression strain as compared to the vector control in qRT-PCR analysis whereas disruption of *p18* reduced its expression to 0.09-fold (Figure 31B).

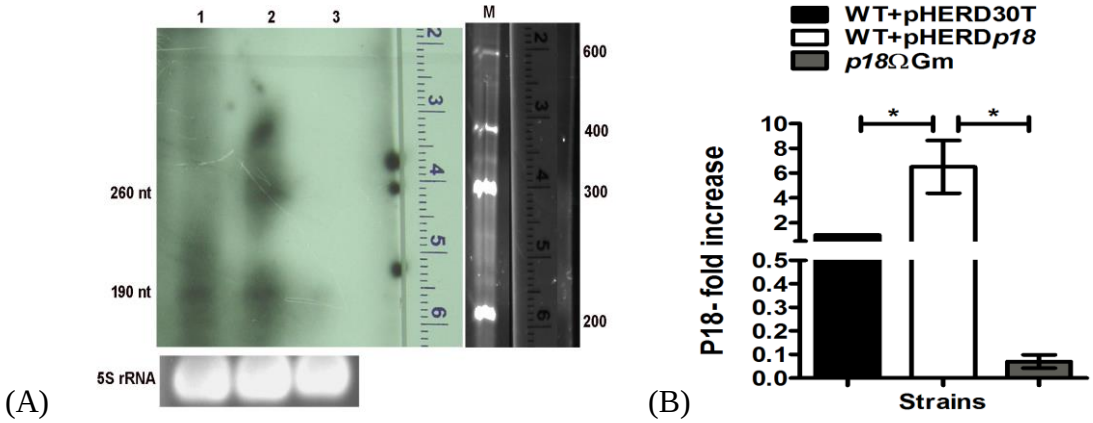

Figure 31: *p18* expression in modified strains.
Total RNA isolated from stationary phase grown cultures was (A) Blotted onto nylon membrane and hybridized with ds P18 DNA probes. Lane 1-*p18*ΩGm; Lane 2-WT+pHERD*p18*; Lane 3-WT+pHERD30T. 5S rRNA is used as the loading control. (B) Converted into cDNA and analyzed by relative qRT-PCR. * indicates P value ≤ 0.05. The experiment was repeated twice and each sample was analyzed in triplicates.

4.3.5 Effect of altered levels of P18 on expression of *aprE* and *piv*

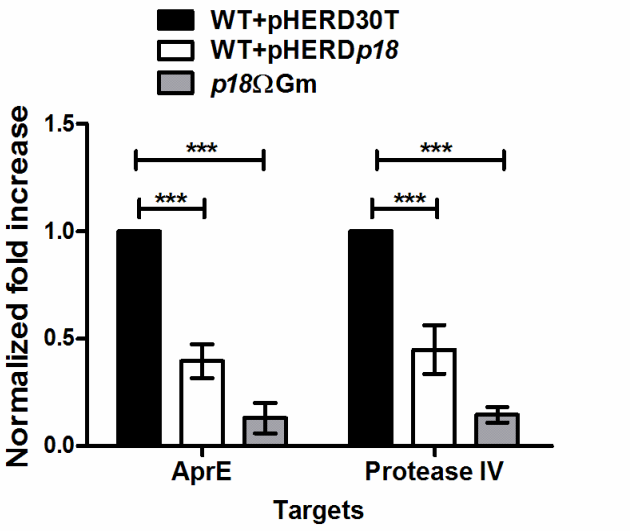

Figure 32: Relative qRT-PCRs assaying the effect of P18 on target mRNAs.
Influence of P18 overexpression (WT+pHERD*p18*) and disruption (*p18*ΩGm) on AprE and Protease IV levels as compared to the vector control (WT+pHERD30T). Each experiment was performed twice and every sample was analyzed in triplicates. Statistical analysis performed using two way ANOVA indicates *** P value ≤ 0.001.

Alkaline protease and protease IV are important virulence factors of *P. aeruginosa* and along with other proteases like elastase A and B have an important role to play in establishing acute infections of *Pseudomonas* (Strateva and Mitov 2011). mRNAs of a secretion protein of alkaline protease, *AprE*, and *PIV* showed potential base pairing with P18 sRNA in IntaRNA program (Figure 26). P18 base paired with *AprE* at its 5'UTR spanning the region from -30 to +16 nucleotides and with protease IV, at +354 to +382 in its coding region. The transcript levels of both the target mRNAs were reduced to ~ 0.14- fold on disruption of *p18* gene in the strain *p18*ΩGm indicating the necessity of this sRNA for their expression. However, overexpression of P18 further down regulated the levels of these proteases in the strain WT+pHERD*p18* when compared to the vector control WT+pHERD30T (Figure 32).

4.3.6 P18 influences alkaline protease and protease IV production

Down regulation of alkaline protease secretion protein E should affect the secretion of alkaline protease into the culture supernatant. With this rationale, activity of the alkaline

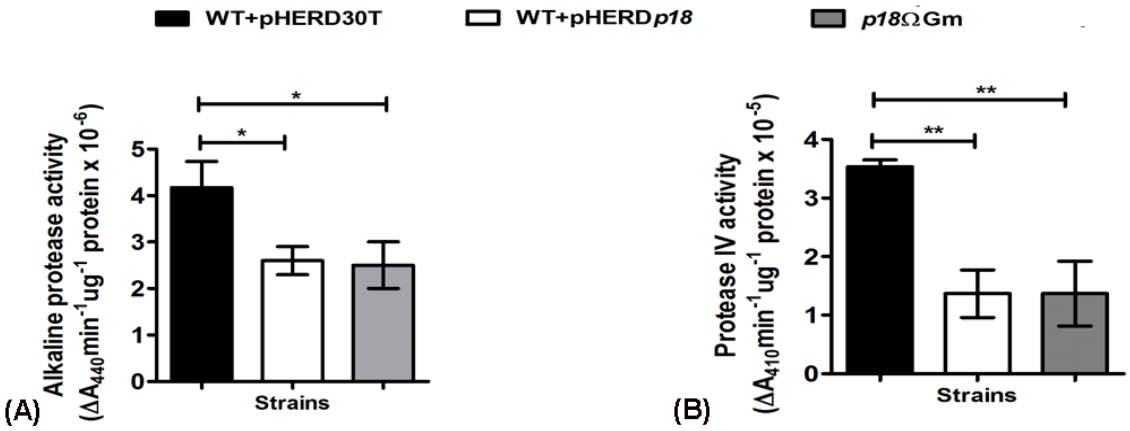

Figure 33: Phenotypic assays of alkaline protease and protease IV.
Spectrophotometric assays for estimation of (A) alkaline protease and (B) protease IV; in supernatants of cultures grown to stationary phase. Activity of the enzymes is represented as increase in the absorbance at respective wavelength/min/µg of protein. Asterisks indicate the data to be statistically significant at P value ≤ 0.05 and P value ≤ 0.01 for * and ** respectively. Each experiment was performed thrice and every sample was analyzed in duplicates.

protease secreted into the culture supernatants was measured by azocasein cleavage method as described in materials and methods. Similarly, a substrate, chromozym PL, specific for lysyl proteases was used to assay the production of protease IV. The secretion of both the proteases was reduced in the disruption strain which corroborated with the trends observed in qRT-

PCR. However the activity of alkaline protease and protease IV was reduced to 40% and 60% respectively (Figure 33) as against the 85% reduction observed in the transcript levels in qRT-PCR (Figure 32). The activity of the proteases in the pHERD*p18* strain was equal to that observed in *p18*ΩGm. Disruption of *p18* reduced the levels of alkaline protease and protease IV as observed in transcriptional and physiological assays indicating the necessity of P18 for the expression of these targets. It was expected that overexpression of P18 should reverse this effect and increase the expression of the proteases. Instead overexpression of P18 also reduced the proteases' expression but to a lesser extent.

Protease IV and alkaline protease are regulated by LasR quorum sensing regulator of *Pseudomonas* at least in two different ways in an indirect manner. 1) Although there is no evidence of a *las* box in the promoter region of these genes (Conibear et al. 2012;Gilbert et al. 2009), LasR directly regulates the expression of *xcp* genes of type II secretion system (Gilbert et al. 2009) that exports protease IV out of the cell (Jyot et al. 2011). Therefore, LasR might regulate the secretion of protease IV to the cell exterior and not its expression per se. 2) The expression of both these proteases is induced under iron deficient conditions by alternate sigma factor PvdS (Shigematsu et al. 2001;Conibear et al. 2012), which itself is under the direct control of LasR (Gilbert et al. 2009). Therefore, it appears that expression of alkaline protease and protease IV is regulated by major sigma factors and transcriptional regulators either directly or in an indirect manner. An *in silico* analysis indicated a very extensive base pairing of P18 sRNA with *LasR* mRNA in its coding region towards the 3' end by IntaRNA program (Figure 34).

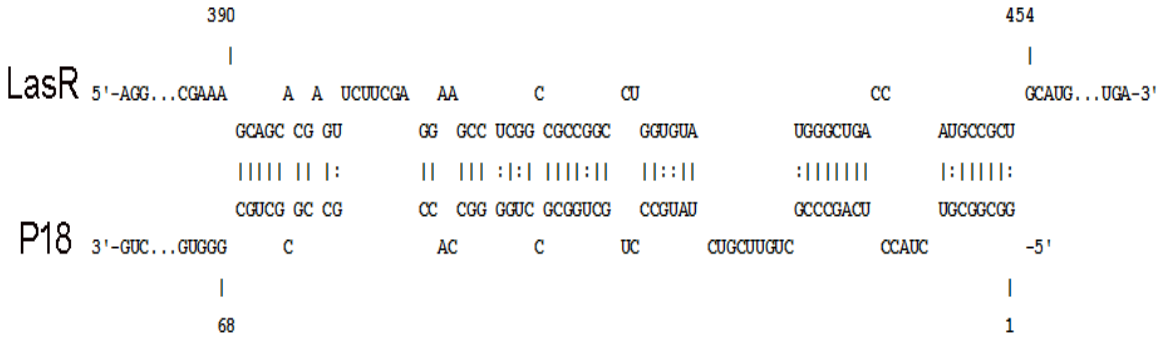

Figure 34: RNA-RNA interaction between LasR and P18 predicted by IntaRNA.

Above observations lead to a speculation that these proteases are regulated by P18 via a major regulator like LasR and therefore are indirect targets of the sRNA.